Journal of Materials Science, Volume 56, February 2021, pp. 3874-3886
DOI: 10.1007/s10853-020-05449-x

High Photocatalytic Activity of Cu_2O embedded in hierarchically hollow SiO_2 for Efficient Chemoselective Hydrogenation of Nitroarenes

Zhengliang Yin,[a] Yingguan Xiao,[a] Xiong Wan,[a] Ying Jiang,[b] Gang Chen,[a]* Qingye Shi,[a] Shunsheng Cao,[a]*

[a] *Research School of Polymer Materials, School of Materials Science and Engineering, Jiangsu University, Zhenjiang 212013, China*

[b] *School of Water, Energy and Environment, Cranfield University, Bedford MK43 0AL, UK*

Abstract

Photocatalytic organic conversion is a crucial process in the hydrogenation of nitroarenes, but harsh reaction conditions such as long reaction time, high hydrogen pressure, and organic medium still need to be considerably overcome under visible-light irradiation. Here, we have constructed a transition metal oxide photocatalyst by embedding low-cost Cu_2O with strong visible-light absorption into hierarchically hollow SiO_2 sphere (SiO_2-Cu_2O@SiO_2) that can suppress the escape of photogenerated atomic hydrogen and promote the contact probability between hydrogen atom and nitroarene molecules due to confinement effect. Remarkably, the SiO_2-Cu_2O@SiO_2 photocatalyst can exhibit efficient chemoselectivity toward the hydrogenation of various nitroarenes in an aqueous system at ambient conditions, successfully working out the requirement of strict hydrogenation conditions, especially for organic medium over almost all of the reported photocatalysts. Notably, quantitative aniline can be produced for the visible-light catalytic reduction of nitroarenes, suggesting a considerable potential for industrial applications.

Graphic abstract

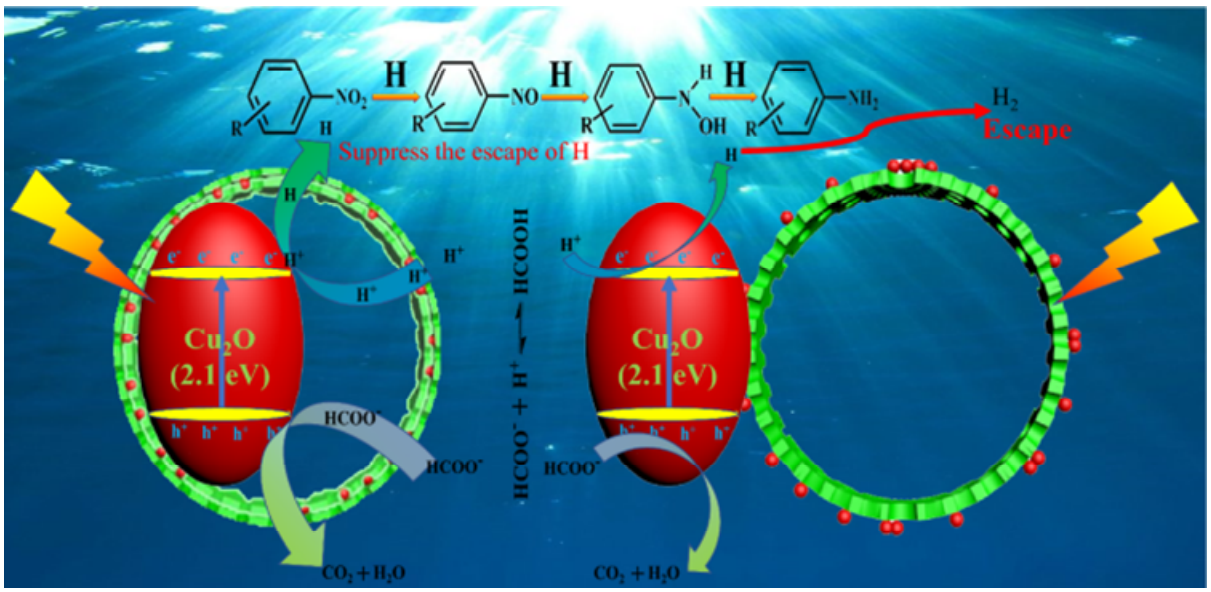

1. Introduction

The selective hydrogenation of nitroarenes over efficient catalysts is the method of choice for the production of anilines and their derivatives that are extremely important intermediates for the manufacture of chemicals, fuels, agrochemicals, and pharmaceuticals [1,2,3,4]. Although supported metal catalysts present efficient performance for the reduction of nitroarenes, the inevitable by-products severely limit their practical applications due to stepwise reduction of nitroarenes [4,5,6]. Furthermore, it is a big challenge to realize perfect chemoselectivity of nitroarene over most of the supported metal catalysts when a nitroarene molecule consists of one or more reducible groups (*e.g.,* − OOH, − Cl, − C = O, etc.) [7, 8]. In particular, the reported heterogeneous catalysts simultaneously induce the undesirable elimination of these functional groups due to harsh reaction conditions such as high temperature or high hydrogen pressure[2, 4, 9,10,11,12,13], which subsequently affects downstream chemical synthesis processes. Therefore, it is of significant interest for

commercial and academic research to construct novel catalysts which catalyze hydrogenation reactions under mild reaction conditions and with high chemoselectivity.

The use of photocatalytic hydrogenation process to promote the selective reduction of nitroarenes has been considered as a promising strategy to decrease the production of undesirable by-products and manifest an efficient chemoselectivity under ambient conditions [14]. To date, many photocatalysts were reported for their abilities of selective reduction of nitroarenes to corresponding amines including rGO/g-C_3N_4 [15], TiO_2 [16], Pd/TiO_2 [17], hybrid Au–Ag [18], and noble metal/HNb_3O_8 [19]. Unfortunately, these photocatalysts exhibited low quantum efficiencies under visible-light illumination, even when noble metal (Au, Pt, or Pd) was employed as co-catalyst to activate and decompose hydrogen toward the reduction of nitroarenes, especially involving in hydrogen transfer steps [19]. Notably, the dependence of organic medium for the hydrogenation of nitroarenes also limits their further applications [9, 19,20,21,22]. Although several works attempted to use an aqueous system to hydrogenate nitroarenes [2, 16, 23,24,25,26], such reactions required more strict conditions: long reaction time (> 12 h) [24, 25], high temperature (> 50 °C) [2, 24], and high energy light sources (UV light) [2, 26]. T herefore, the use of abundantly available transition metals is especially attractive to replace rare and high-cost noble metals in catalysts for the hydrogenation of nitroarenes if similar catalytic performance can be achieved under mild reaction conditions.

To address this challenge, we devise and prepare a novel visible-light photocatalyst by encapsulating low-cost Cu_2O into hierarchically hollow SiO_2 sphere without visible-light absorption (named as SiO_2-Cu_2O@SiO_2), exhibiting the efficient chemoselective hydrogenation of various nitroarenes. More importantly, we present the first application of transition metal oxide photocatalyst for directly hydrogenating nitroarenes to obtain functionalized amines in an aqueous medium under ambient conditions. Experimental data

suggest that high activity and chemoselectivity can be ascribed to confinement effect and the embedded Cu_2O.

2. Experimental section

2.1 Materials

Cupric nitrate, styrene, $K_2S_2O_8$, o-chloronitrobenzene (o-NCB), p-nitrobenzoic acid (p-NBA), and inter-nitroacetophenone (i-NAP) were purchased from Sinopharm Chemical Reagent Co., LtdS (China), and styrene was pretreated to remove polymerization inhibitors according to our previous works[27, 28]. Other chemicals were available from J&K scientific Ltd.

2.2 Cupric ions immobilization

Cationic polystyrene sphere (CPS) @SiO2 core/shell spheres prepared by referring previous publications [27, 28] were used as templates to immobilize cupric ion via an impregnation method [29]. Typically, the as-synthesized CPS@SiO_2 spheres and the required amount of cupric nitrate were dispersed into deionized water, after stirring for 24 h, and the solution was evaporated and dried under vacuum overnight at 50 °C, producing CPS@SiO_2-Cu^{2+} composite.

2.3 Preparation of SiO_2-Cu_2O@SiO_2 confined photocatalyst

The CPS@SiO_2-Cu^{2+} (3 g) was dispersed into ethanol by mechanical stirring, and then, TEOS (1 g) was added into this system at 50 °C. After that, the reactive system was further kept for 6 h to allow a saturated adsorption of tetraethyl orthosilicate **(**TEOS) on the surface of CPS@SiO_2-Cu^{2+}, and then, ammonia (3 mL) was added into this system to allow sol–gel process to occur, preparing CPS@SiO_2-Cu^{2+}@SiO_2 particles. After removing CPS at 450 °C, SiO_2-CuO@SiO_2 was formed. Finally, the resulting particles were reduced to Cu, Cu_2O, CuO using excess H_2 flow, Ar/H_2 (V:V = 9:1), and air atmosphere [30, 31], forming SiO_2-Cu@SiO_2, SiO_2-Cu_2O@SiO_2, and SiO_2-CuO@SiO_2 confined photocatalysts, respectively. For

performance comparison, surface-supported Cu_2O (SiO_2-Cu_2O) was prepared by directly immobilizing Cu_2O onto the surface of hierarchically hollow SiO_2 via the same process.

2.4 Characterization

The architecture and morphology of the SiO_2-Cu_2O@SiO_2 photocatalyst were measured by transmission electron microscope (TEM), scanning electron microscope (SEM), and STEM mapping. Its surface area and pore distribution were investigated by Brunauer–Emmett–Teller (BET)/Barrett–Joyner–Halenda (BJH) methods through a micromeritics ASAP 2460. In addition, X-ray diffraction (XRD), X-ray photoelectron spectroscopy (XPS), and UV–Vis spectroscopy were used to characterize crystal, bonding energy, and light absorption of the photocatalyst.

2.5 Photoelectrochemical properties of SiO_2-Cu_2O@SiO_2

The preparation of electrode: SiO_2-Cu_2O@SiO_2 powder (5 mg), was dispersed in mixture solution (ethanol: 1 mL; glycol: 1 mL). After that, 20 μL dispersion sample was withdrawn, then coated in ITO glass (1 cm^2), and dried in the oven at 80 °C.

The photocurrent was performed on a standard three electrode cell with a working electrode, a Pt wire as the counter electrode, and a saturated calomel electrode using 0.5 M Na_2SO_4 as electrolyte under light illumination through electrochemical workstation (CHI-660E electrochemical analyzer, China). The potential of photocurrent measurement is + 0.2 V. Electrochemical impedance spectroscopy (EIS) was carried out at the open-circuit potential in dark. Incidentally, the reported data are the average of three measurements.

2.6 Photocatalytic reduction of nitroarene

Catalyst (50 mg), nitroarenes (0.25 mg/mL: o-NCB and p-NBA), and formic acid (2.7 mg) were poured into a 10 ml deionized water solution. After bubbling nitrogen for 30 min, the sealed reactor was placed in a thermostatic water bath at 25 °C and illuminated under visible

light ($\lambda > 400$ nm). The photocatalyst was filtrated through a syringe filter, and the solution was detected by high-performance liquid chromatography (HPLC). Incidentally, the initial concentration of i-NAP (0.025, 0.05, 0.1 mg/ml) was used because of its poor solubility, and the amount of formic acid decreases accordingly.

3. Results and discussion

3.1 The synthesis and morphology of SiO_2-Cu_2O@SiO_2 photocatalyst

The novel cuprous oxides (Cu_2O) confined photocatalyst was prepared in a three-step procedure, as shown in Fig. 1a. Firstly, cupric ions (Cu^{2+}) are deposited on the surface of CPS@SiO_2 sphere via electrostatic attraction, forming CPS@SiO_2-Cu^{2+} composite. Secondly, CPS@SiO_2-Cu^{2+} was coated by outer SiO_2 through the hydrolysis and condensation of TEOS. After removal of CPS template at high temperature under a H_2/Ar atmosphere, SiO_2-Cu_2O@SiO_2 visible-light photocatalyst was formed. A ~ 9.6 wt% copper in the sample was revealed by inductively coupled plasma optical emission spectrometry (ICP-OES) measurement.

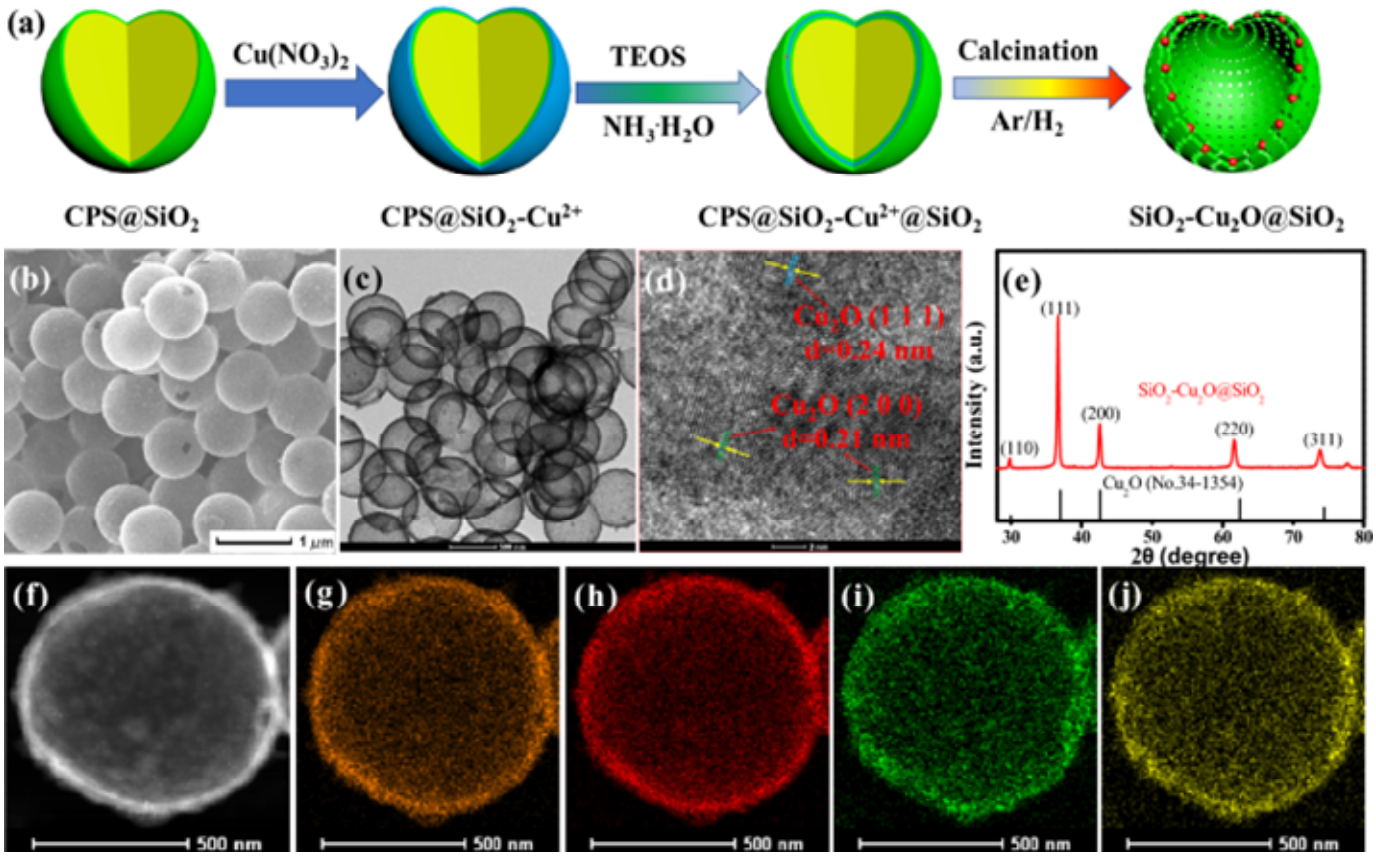

Figure 1. a The preparation process of the SiO_2 Cu_2O@SiO_2 photocatalyst.

b SEM, **c** TEM, **d** HRTEM, **e** XRD, and **f** STEM mapping **g** Si, **h** O, **i** Cu, and **j** C

Figure 1b shows that the as-synthesized SiO_2-Cu_2O@SiO_2 photocatalyst has a spherical morphology and a hollow feature. TEM image further ascertains the hollow structure of this particle and further reveals that a number of dark particles are observed (Fig. 1c). Using high-resolution TEM (HRTEM) to focus on a dark particle structure, it reveals clear lattice fringes with 0.210 nm (200) and 0.24 nm (111) spacing (Fig. 1d), which can be ascribed to the facets of Cu_2O[28]. To further determine bulk phase feature, the sample was characterized by XRD. The diffraction peaks located at 30.0, 37.0, 42.6, 62.4, and 74.4° (Fig. 1e) can be attributed to the crystal facets of Cu_2O (JCPDS No. 34–1354) [28]. The energy-dispersive X-ray spectroscopy (EDX) result confirms the existence of C, O, Cu, and Si elements (Figure S1). STEM mapping clearly displays that Cu signal exhibits the same spherical morphology as the signals of Si and O have (Fig. 1g-i), indicating the good

size distribution of Cu_2O particles. Notably, the elemental profiles of SiO_2-Cu_2O@SiO_2 sample evidently display that Cu signal appears between Si signal and O signal (Fig. 2), which is clearly different from the comparative signal of Cu resulting from surface-supported Cu_2O because the signal of Cu also is observed at both ends of silicon and oxygen (Figure S2). BET isotherm for SiO_2-Cu_2O@SiO_2 demonstrates a type IV with a weak hysteresis loop (Figure S3). Furthermore, BET isotherm and BJH pore size distribution show that the SiO_2-Cu_2O@SiO_2 holds a porous nature with a high surface area of 98.6 m^2/g (Figure S3), facilitating reactant/product diffusion into/from the photocatalyst. All these results confirm that Cu_2O embedded into hierarchically hollow silica support has been prepared through calcination under an Ar/H_2 atmosphere [29].

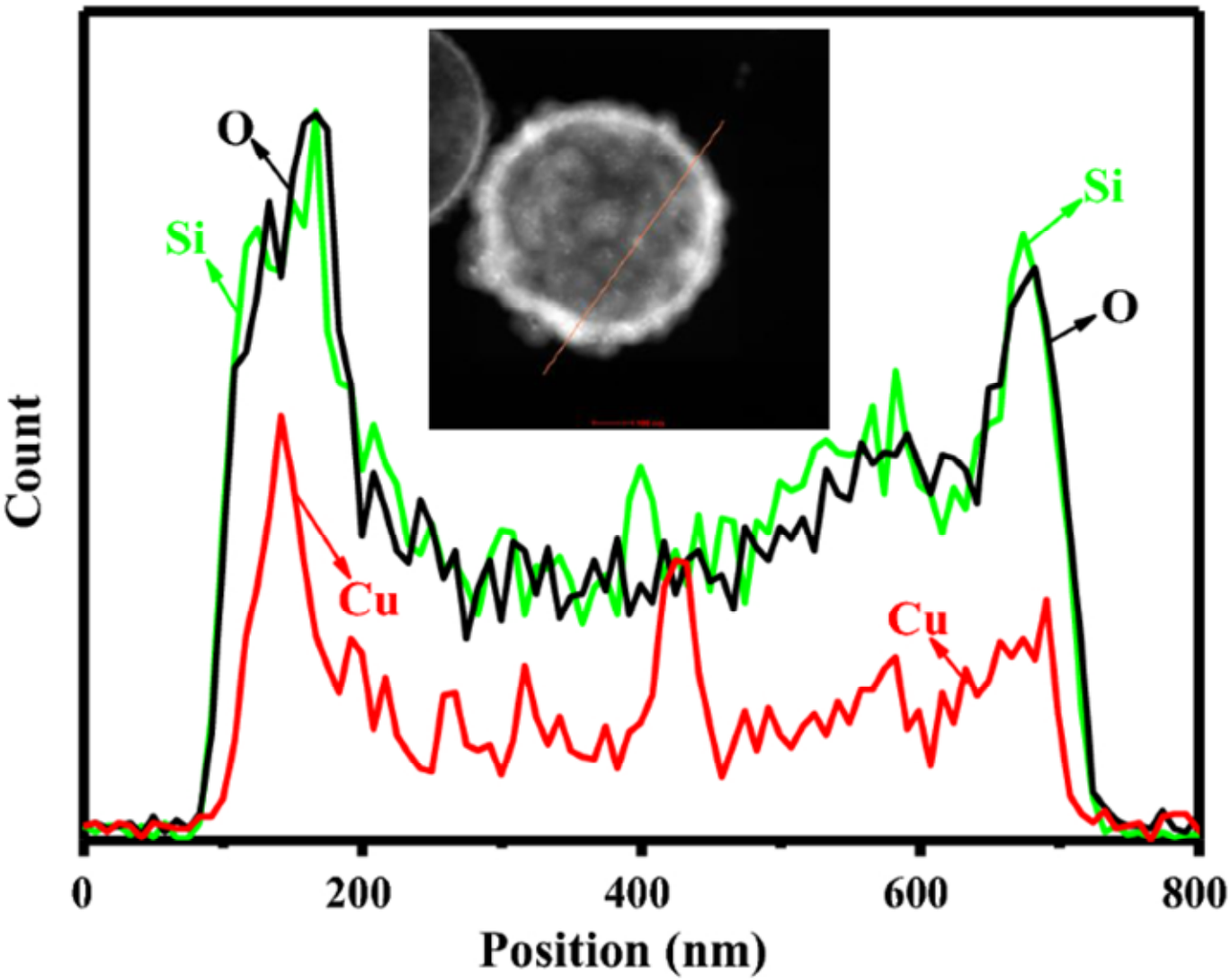

Figure 2. Elemental profiles (Si, O, and Cu elements) of the as-synthesized SiO_2-Cu_2O@SiO_2 sample

3.2 Bonding environment of SiO_2-Cu_2O@SiO_2 photocatalyst

The bonding environment of the photocatalyst was ascertained using XPS measurement. Figure 3 shows the existences of Cu, O, C, and Si. Peaks at 933.6 and 953.75 eV are ascribed to Cu $2p_{3/2}$ and Cu $2p_{1/2}$, respectively [32,33,34]. Unfortunately, it is very difficult in determining the peaks resulting from Cu_2O or metal Cu due to a small difference in Cu 2p core peak [32]. Alternatively, using Cu [LMM] Auger peak is more reliable confirming the chemical status. The result shows that Auger spectra at 570.0 eV are attributed to Cu_2O other than metal Cu because of the relatively low band energy (568 eV) of Cu [32, 35]. This result is in agreement with the measurements by XRD and HRTEM. Figure 3d shows that peak located at 531.5 eV can be indexed to Cu-O [32], while another peak is attributed to surface OH group [29]. In addition, the XPS spectra of C1s can be fitted to two peaks at 284.58 and 286.38 eV, in which peak at 284.58 eV is assigned to residual carbon during the pyrolysis of CPS template, which serves as a photo-sensitizer to strengthen its visible-light absorption [36].

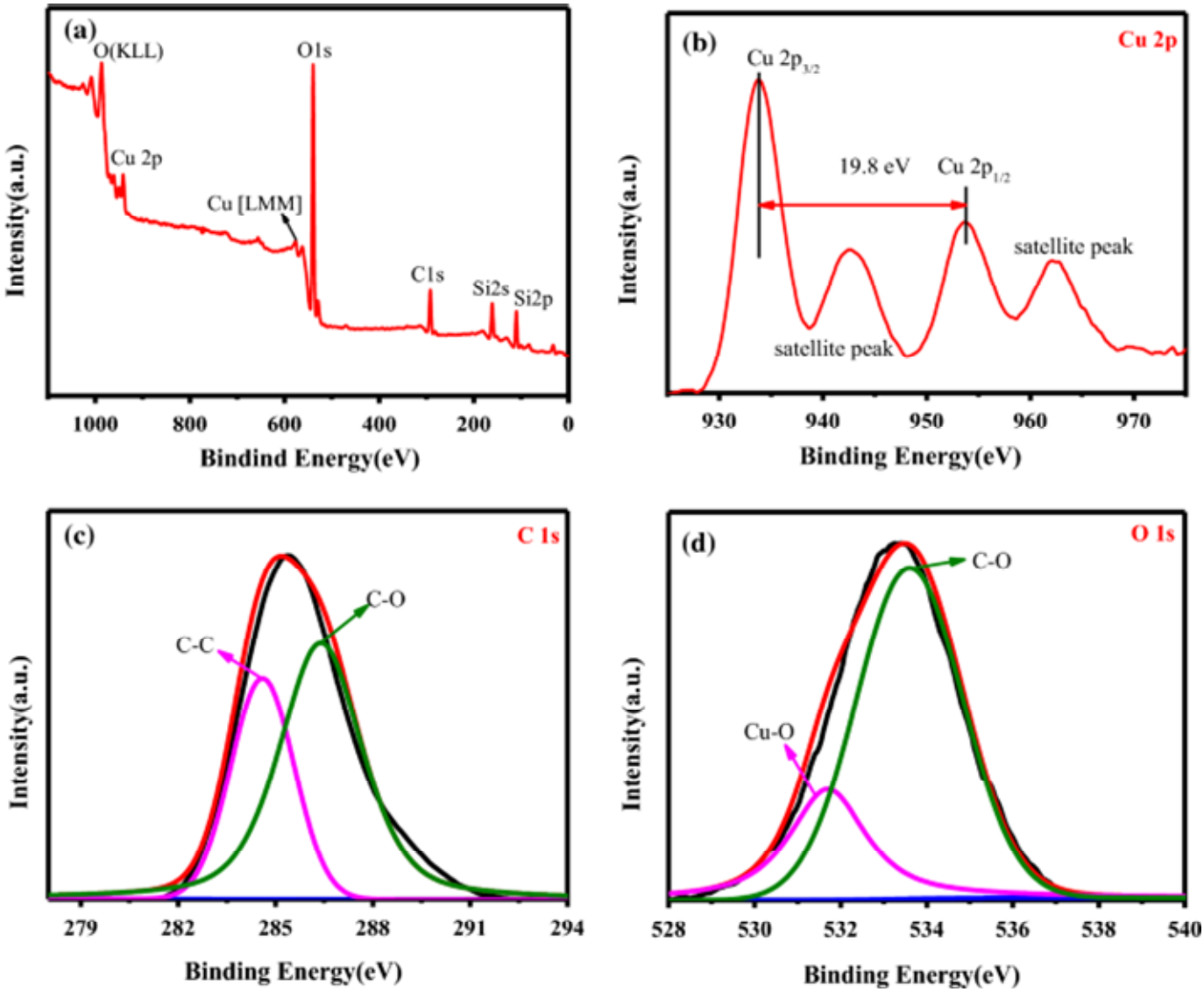

Figure 3. **a** XPS full spectra, **b** Cu 2p, **c** C1s, and **d** O1s of the SiO_2-Cu_2O@SiO_2 sample

Photocatalytic performance of SiO_2-Cu_2O@SiO_2 photocatalyst

Photocatalytic activity was investigated for the chemoselective reduction of o-chloronitrobenzene (o-NCB), p-nitrobenzoic acid (p-NBA), and inter-nitroacetophenone (i-NAP) in an aqueous medium under visible-light illumination. For further comparison, Cu and CuO embedded into hierarchically hollow SiO_2 sphere were synthesized and characterized by XRD (Figure S4), forming SiO_2-Cu@SiO_2 and SiO_2-CuO@SiO_2 confined photocatalysts, responsively. At the initial o-NCB concentration (0.25 mg/mL), after 3-h reaction in an aqueous medium, the catalytic performance of SiO_2-Cu@SiO_2 appears to be poor with low conversion rate, chemoselectivity, and yield of o-NCB (~ 81%), as summarized in Table S1.

When higher initial concentration (1.0 mg/mL) is used, the catalytic activity of SiO_2-Cu@SiO_2 deteriorates further (Table 1) because Cu is a metal other than a semiconductor [37], indicating poor chemoselective hydrogenation of nitroarenes. Similar chemoselectivity (~ 77%) over SiO_2-CuO@SiO_2 photocatalyst is achieved in the hydrogenation of o-NCB, particularly at higher initial o-NCB concentrations (0.5 or 1.0 mg/mL) (Table 1, S2). By contrast, the as-synthesized SiO_2-Cu_2O@SiO_2 photocatalyst exhibits the best photocatalytic performance (> 99%) including conversion, chemoselectivity, and yield (Table S1) compared with previous two catalysts. This catalyst continues to achieve high chemoselectivity (> 99%) of o-NCB even when initial concentration of o-NCB is increased to 0.5 or 1.0 mg/mL (Table 1, S2), suggesting superior photocatalytic performance of the SiO_2-Cu_2O@SiO_2 photocatalyst. These experimental results show that Cu_2O plays a key role in achieving excellent chemoselectivity, which is strongly confirmed by hydrogenating other typical nitroarenes. As shown in Table S1, the SiO_2-Cu_2O@SiO_2 photocatalyst presents a superior chemoselectivity (100%) of p-nitrobenzoic acid (p-NBA), far beyond the comparative values of p-NBA when compared with results achieved by SiO_2-CuO@SiO_2 (66.8%) and SiO_2-Cu@SiO_2 (66.1%). When the doubled and four-folded concentration of p-NBA is used, chemoselectivity over the sample still is as high as > 99%, while extremely low chemoselectivity (43 – 60%) is observed for other two controls (Table 1). The performance advantage of SiO_2-Cu_2O@SiO_2 photocatalyst is further confirmed by hydrogenating inter-nitroacetophenone (i-NAP) under the same conditions (Tables 1, S1, 2). The best photocatalytic performance of SiO_2-Cu_2O@SiO_2 is mainly responsible for the highest charge separation efficiency. The maximum value of photocurrent intensity and the smallest semicircle in the Nyquist plots also reveal higher charge separation of the as-synthesized photocatalyst than that of SiO_2-CuO@SiO_2 (Figure S5**)** [38, 39], while Cu in the SiO_2-Cu@SiO_2 sample is a metal other than a semiconductor. Additionally, we further investigated the effect of the addition amount of cupric nitrate on the hydrogenation of nitroarenes. The result shows that the amount of cupric nitrate has little effect on the hydrogenation of o-NCB (Figure S6). This performance of SiO_2-Cu_2O@SiO_2 photocatalyst

meets the requirements for mild reaction conditions and out-performs over many previously reported photocatalysts for the chemoselective reduction of nitroarenes (Table S3) [9, 22, 25, 40].

Table 1 The catalytic activity of photocatalysts toward the reduction of nitroarenes in aqueous system

Nitroarene	SiO_2-Cu_2O@SiO_2			SiO_2-CuO@SiO_2			SiO_2-Cu@SiO_2		
	Conv (%)	Selec (%)	Yield (%)	Conv (%)	Selec (%)	Yield (%)	Conv (%)	Selec (%)	Yield (%)
o-NCB (1.0 mg/ml)	100	99.4	99.0	43.1	44.7	44.4	68.9	67.5	67.1
p-NBA (1.0 mg/ml)	100	99.8	99.2	43.9	44.0	43.8	46.7	48.0	47.8
i-NAP (0.1 mg/ml)	100	99.8	99.4	45.8	40.4	40.2	39.7	37.8	37.6

3.3 Role of confinement effect on the hydrogenation of nitroarenes

The photocatalytic hydrogenation of nitroarenes was further investigated to deeply understand the role of confinement effect. For comparison, Cu_2O was directly deposited on the surface of hierarchically hollow SiO_2 spheres, preparing surface-supported photocatalyst (SiO_2-Cu_2O, Figures S7, 8). Table 2 shows that the SiO_2-Cu_2O exhibits a chemoselectivity and yield (~ 91%) for the hydrogenation of o-NCB, while a similar performance is observed toward the photocatalytic hydrogenation of p-NBA and i-NAP. By contrast, the confined Cu_2O (SiO_2-Cu_2O@ SiO_2) holds excellent conversion, chemoselectivity, and yield (> 99%) for the hydrogenation of o-NCB. Even for the hydrogenations of p-NBA and i-NAP, chemoselectivity still is as high as > 99%, beyond the values (90 ~ 94%) of p-NBA and i-NAP

over surface-supported Cu_2O photocatalyst. Two photocatalysts have similar Cu_2O loading and light absorption characteristic (Figure S7); therefore, the distinct photocatalytic performance can be ascribed to confinement effect and Cu_2O aggregation in the surface-supported SiO_2-Cu_2O photocatalyst (Figure S8).

Table 2 The comparative hydrogenation of nitroarenes over two photocatalysts

Nitroarenes	SiO_2-Cu_2O@SiO_2			SiO_2-Cu_2O		
	Conv (%)	Selec (%)	Yield (%)	Conv (%)	Selec (%)	Yield (%)
o-NCB (1.0 mg/ml)	100	99.4	99.0	93.4	91.7	91.1
p-NBA (1.0 mg/ml)	100	99.8	99.2	92.7	90.4	90.0
i-NAP (0.1 mg/ml)	100	99.8	99.4	96.7	95.0	94.6

3.4 Kinetics and chemical reaction stoichiometry

The hydrogenation of o-chloronitrobenzene (o-NCB) over two photocatalysts was investigated at a variety of temperatures for different times to understand the influence of temperature on the apparent rate constant (k_{app}) based on Eq. (1) [27, 41]:

$$\ln(C/C_0) = - k_{app} t \qquad (1)$$

here C_0 and C are the reactant and initial concentration of nitrobenzene, respectively. Fig. 4 indicates that the k_{app} enhances with increasing temperature, implying that o-NCB molecule can freely access the confined photocatalyst. Based on the Arrhenius equation (2):

$$\ln k_{app} = \ln A - E_a/RT \qquad (2)$$

where E_a is the energy of activation, A is the pre-exponential factor, and R is the general gas constant. Figure 4 demonstrates that a high E_a (97.7 kJ/mol) over the confined SiO_2-Cu_2O@SiO_2 sample is obtained toward the hydrogenation of o-NCB, which is twice higher than value (40.6 kJ/mol) over surface-supported SiO_2-Cu_2O photocatalyst due to the higher diffusional limitation resulting from confinement effect. Notably, with the increase in the reaction time, higher conversion (100%) is obtained due to confinement effect (Figure S9).

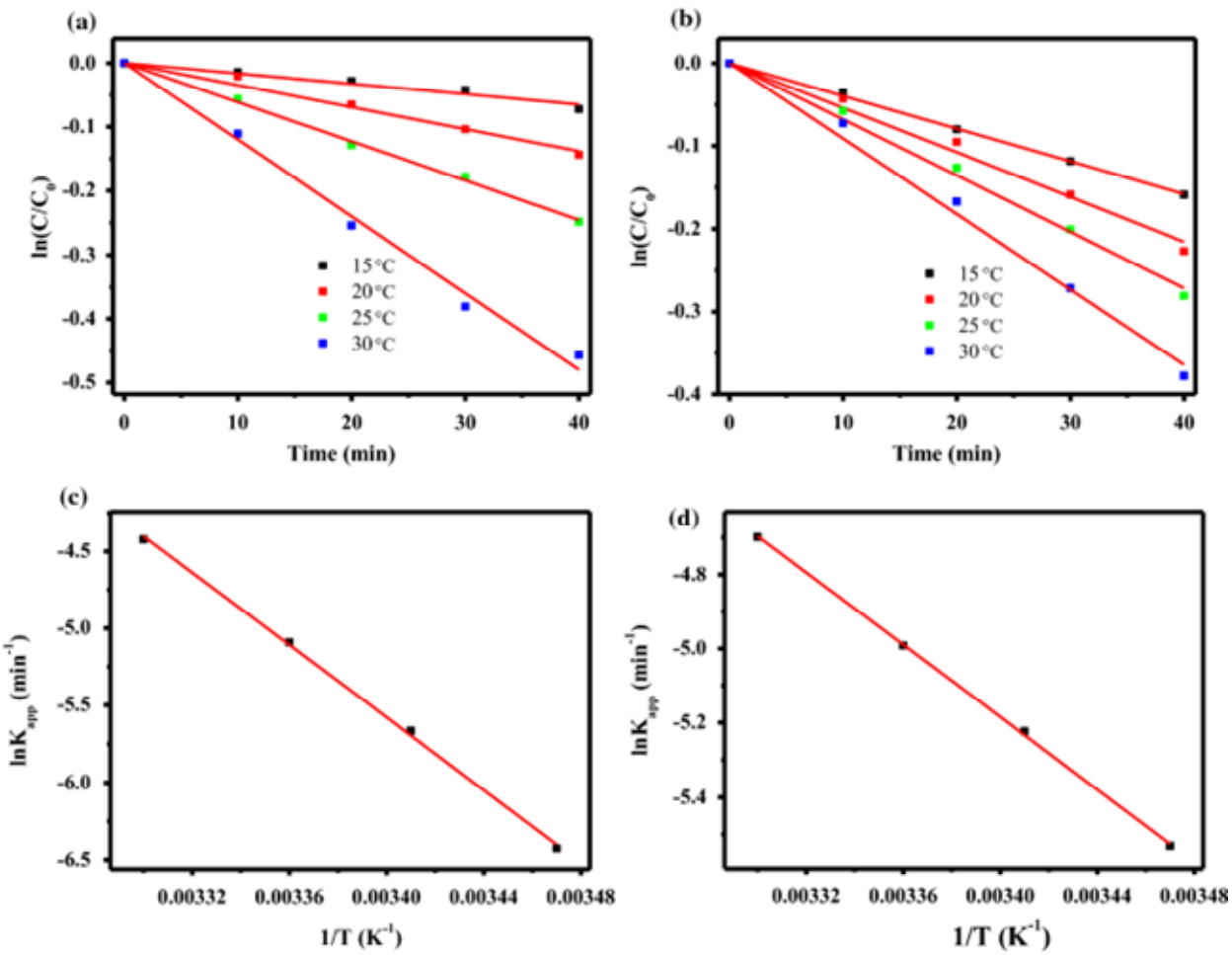

Figure 4. Plot of ln(C/C_0) versus t (min) and Arrhenius plot of ln k*app* versus 1/T (K^{-1}) for hydrogenation of o-NCB over SiO_2-Cu_2O@SiO_2 (**a**,**c**) and SiO_2-Cu_2O (**b**, **d**) samples

To investigate chemical reaction stoichiometry, we measured yields on the photocatalytic reduction of three nitroarenes at various concentrations by HPLC. The corresponding aniline is almost quantitatively produced for hydrogenating nitroarenes in an aqueous medium at room temperature, which fairly agrees with the standard curves of commercial amines (Figure S10).

3.5 Catalyst stability

Cycle experiment was performed using o-chloronitrobenzene (o-NCB) as a hydrogenation reaction model through the investigation of chemoselectivity and yield for three consecutive tests over two photocatalysts. Photocatalyst after each reaction run can be readily separated via centrifugation and washed from reaction system and then reused for the next test under the same conditions. It is universally accepted that the photocorrosion and aggregation of Cu_2O are easy to happen under light irradiation [37], which is ascertained by surface-supported SiO_2-Cu_2O with larger Cu_2O nanoparticles (Figure S8). Figure S11 shows that the chemoselectivity and yield of o-NCB for the surface-supported SiO_2-Cu_2O are ~ 91.6% after 3 h in the first run, and a clearly decreased chemoselectivity (~ 71.3%) is observed in the second run. In particular, a sharply decreased chemoselectivity with low yield (~ 38.6%) is found after the third test. By contrast, the confined Cu_2O (SiO_2-Cu_2O@SiO_2) photocatalyst remains high chemoselectivity and yield (> 90.0%) even after three cycles. Notably, the aggregation of the embedded Cu_2O does not happen and the hollow structure of SiO_2 support remains well (Figure S12), indicating that the stability of embedded Cu_2O has been significantly increased due to confinement effect.

3.6 Hydrogenation mechanism of nitroarenes

To figure out the type of catalytic reaction (photocatalysis or thermal catalysis) during the chemoselective hydrogenation of nitroarenes, comparative experiment without light irradiation (in the dark) was performed. Figure 5 shows that the conversion of o-NCB is 6.5% without light irradiation at 20 °C, while the conversion of p-NBA and i-NAP is as low as < 5%.

Notably, although an enhanced conversion (< 40%) of three nitroarenes is observed when higher temperature (35 °C) is used, a negligible chemoselectivity (< 2%) is observed, strongly confirming that the excellent chemoselectivity of nitroarene is completely attributed to photocatalysis other than thermal catalysis over the as-synthesized SiO_2-Cu_2O@SiO_2 catalyst. In addition, hierarchically hollow SiO_2 spheres were also used as catalyst for the hydrogenation of o-NCB in pure water under visible-light irradiation, and the experimental result shows that corresponding amine is not detected by HPLC (Figure S13), indicating that the hydrogenation of nitroarenes does not happen under visible-light irradiation because SiO_2 is nonconductor [38].

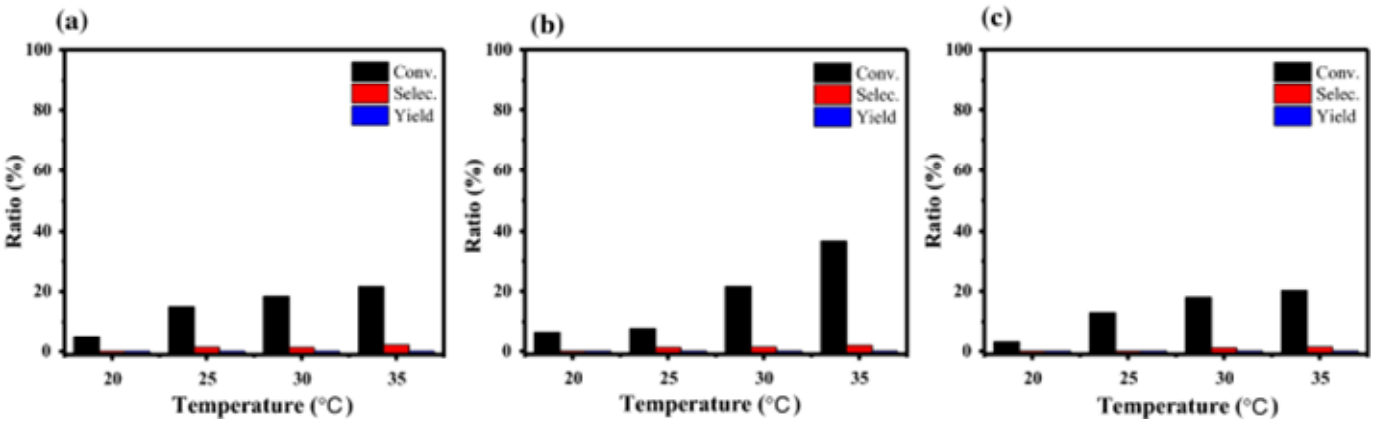

Figure 5 The conversion, chemoselectivity, and yield of o-NCB in dark under the same conditions

To further understand the role of light source, a series of single wavelength (λ = 405, 420, 435, 550 nm) were used to drive the hydrogenation of nitroarenes over the confined Cu_2O (SiO_2-Cu_2O@SiO_2) photocatalyst. Figure 6 shows that high chemoselectivity (~ 86.5%) and yield (~ 86.1%) of three nitroarenes are achieved under single-wavelength irradiation (λ = 405 nm), even when longer wavelength light (λ = 550 nm) is used, and the effective hydrogenation (~ 46.0%) of o-NCB still is observed due to the strong and wide visible-light absorption of the SiO_2-Cu_2O@SiO_2 photocatalyst (Fig. 6d). All these results confirm that Cu_2O is considered as a sole photocatalyst for the excellent chemoselective reduction of nitroarenes under visible light.

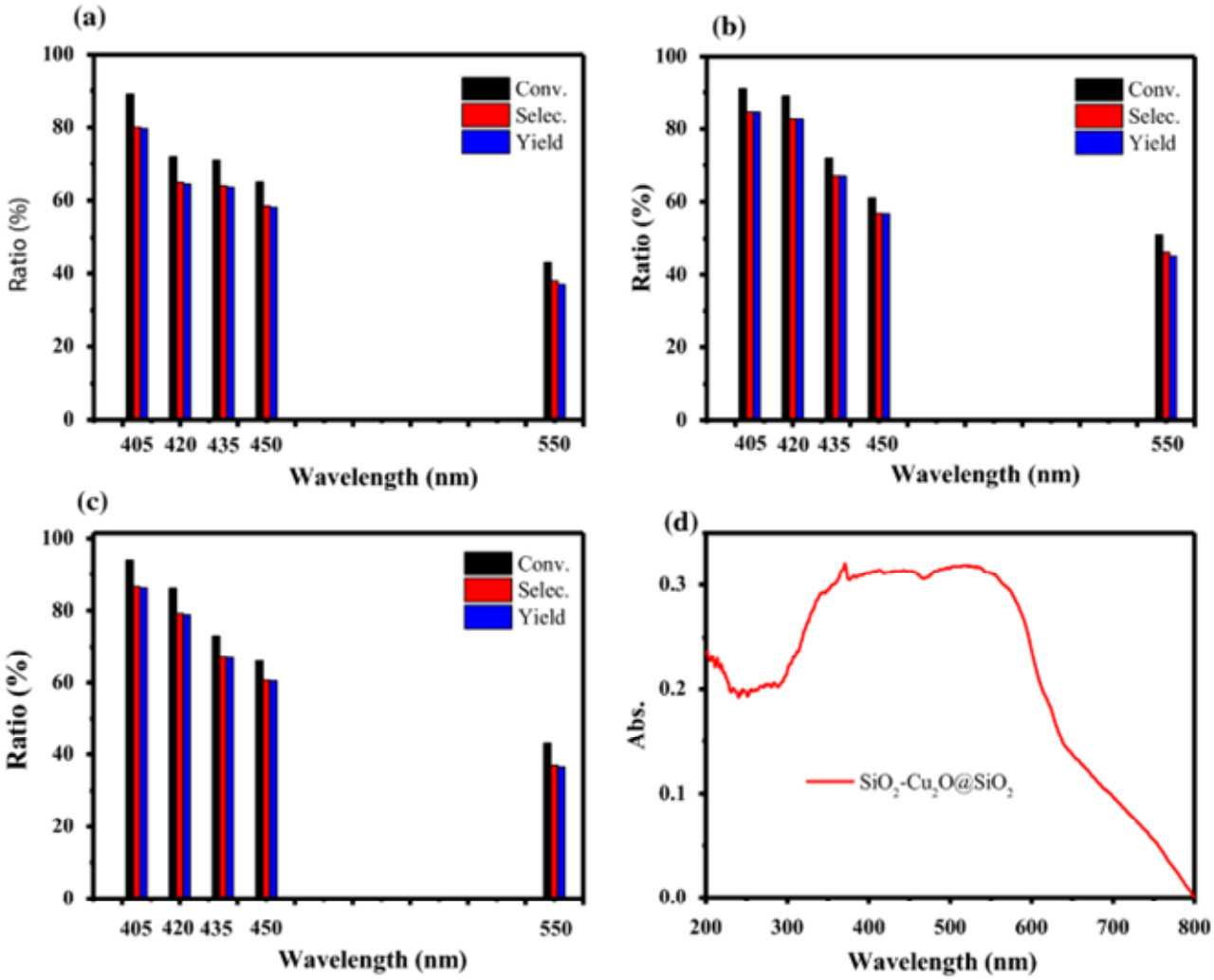

Figure 6. The conversion, selectivity, and yield of o-NCB **(a)**, p-NBA **(b)**, and i-NAP **(c)** under single-wavelength irradiation, and **(d)** UV–Vis spectra of the SiO_2-Cu_2O@SiO_2 sample

Based on the experimental results and the intermediates of nitroarenes through MS spectra, a hydrogenation mechanism of nitroarene is proposed in this study, as shown in Fig. 7. Under visible-light irradiation, Cu_2O is easy to be excited and produces a number of charge pairs due to its band gap (2.0–2.2 eV) [32, 37, 40, 42] and strong visible-light absorption (Fig. 6d). Hydrion (H^+) resulting from formic acid captures photogenerated electrons to produce atomic hydrogen; at the same time, the photogenerated hydrogen atom is transferred to nitroarene molecules, stepwisely forming nitrosobenzene, hydroxylamine and corresponding aniline, while formate species are oxidized by holes [43, 44]. During the hydrogenation process of nitroarene, one part of the photogenerated atomic hydrogen over

surface-supported Cu_2O (SiO_2-Cu_2O) can be transferred to nitroaromatic molecules, while the other parts of atomic hydrogen are easy to be escaped to form H_2, resulting in the low chemoselective hydrogenation of nitroarenes. Notably, the escape of atomic hydrogen over the confined Cu_2O (SiO_2-Cu_2O@SiO_2) will be significantly suppressed because atomic hydrogen is produced within a confined space of hierarchically hollow SiO_2 sphere, leading to excellent chemoselective hydrogenation of nitroarenes.

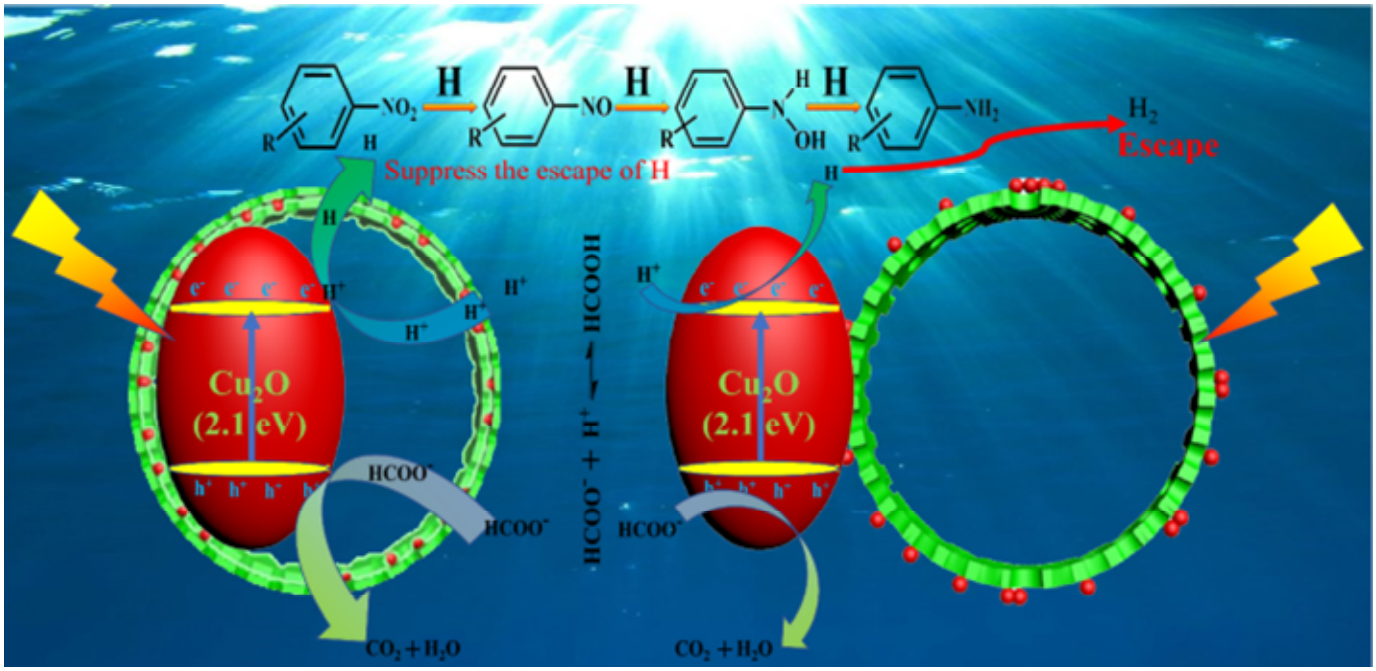

Figure 7. The hydrogenation mechanism of nitroarenes over the surface supported and confined Cu_2O photocatalysts

4. Conclusion

In summary, we present a novel transition metal oxide photocatalyst by embedding low-cost Cu2O with strong visible-light absorption into hierarchically hollow SiO2 sphere. The as-synthesized SiO2-Cu2O@SiO2 photocatalyst is able to significantly suppress the escape of photogenerated hydrogen atom and boost the contact probability of hydrogen atom and nitroarene molecules due to confinement effect, leading to the efficient chemoselective hydrogenation of nitroarenes in an aqueous medium under visible-light illumination. Notably,

we present the first application of transition metal oxide photocatalyst for the direct photocatalytic reduction of nitroarenes to produce functionalized amines under ambient conditions, successfully overcoming the requirement of harsh hydrogenation conditions (e.g., high temperature, long reaction time, powerful light source, etc.) for almost all of the reported photocatalysts. Therefore, the design concept of the novel photocatalyst opens a new door in designing efficient visible-light photocatalysts for the selective catalysis of organic conversions by combining confinement effect and low-cost transition metal oxide.

References

1. Wang L, Guan E, Zhang J, Yang J, Zhu Y, Han Y, Yang M, Cen C, Fu G, Gates BC, Xiao F (2018) Single-site catalyst promoters accelerate metal-catalyzed nitroarene hydrogenation. Nat Commun 9:1362

2. Gao R, Pan L, Wang H, Zhang X, Wang L, Zou J (2018) Ultradispersed nickel phosphide on phosphorus-doped carbon with tailored d-band center for efficient and chemoselective hydrogenation of nitroarenes. ACS Catal 8:8420–8429

3. Shen M, Liu H, Yu C, Yin Z, Muzzio M, Li J, Xi Z, Yu Y, Sun S (2018) Room-temperature chemoselective reduction of 3-nitrostyrene to 3-vinylaniline by ammonia borane over Cu nanoparticles. J Am Chem Soc 140:16460–16463

4. Zhou P, Jiang L, Wang F, Deng K, Lv K, Zhang Z (2017) High performance of a cobalt-nitrogen complex for the reduction and reductive coupling of nitro compounds into amines and their derivatives. Sci Adv 3:e1601945

5. Gao R, Pan L, Wang H, Yao Y, Zhang X, Wang L, Zou J (2019) Breaking trade-off between selectivity and activity of nickel-based hydrogenation catalysts by tuning both steric effect and d-band center. Adv Sci 6:1900054

6. Li J, Song S, Long Y, Wu L, Wang X, Xing Y, Jin R, Liu X, Zhang H (2018) Investigating the hybrid-structure-effect of CeO2-encapsulated Au nanostructures on the transfer coupling of nitrobenzene. Adv. Mater 30:1704416

7. Wei H, Liu X, Wang A, Zhang L, Qiao B, Yang X, Huang Y, Miao S, Liu J, Zhang T (2014) FeOx-supported platinum single-atom and pseudo-single-atom catalysts for chemoselective hydrogenation of functionalized nitroarenes. Nat Commun 5:5634

8. Zhang S, Chang C, Huang Z, Li J, Wu Z, Ma Y, Zhang Z, Wang Y, Qu Y (2016) High catalytic activity and chemoselectivity of sub-nanometric Pd clusters on porous nanorods of CeO2 for hydrogenation of nitroarenes. J Am Chem Soc 138:2629–2637

9. Song Y, Wang H, Wang Z, Guo B, Jing K, Li Y, Wu L (2018) Selective photocatalytic synthesis of haloanilines from halonitrobenzenes over multifunctional AuPt/monolayer titanate nanosheet. ACS Catal 8:9656–9664

10. Wang L, Zhang J, Wang H, Shao Y, Liu X, Wang Y, Lewis JP, Xiao F (2016) Activity and selectivity in nitroarene hydrogenation over Au nanoparticles on the edge/corner of anatase. ACS Catal 6:4110–4116

11. Schwob T, Kempe R (2016) A reusable Co catalyst for the selective hydrogenation of functionalized nitroarenes and the direct synthesis of imines and benzimidazoles from nitroarenes and aldehydes. Angew Chem Int Ed 55:15175–15179

12. Gao R, Pan L, Li Z, Zhang X, Wang L, Zou J (2018) Cobalt nanoparticles encapsulated in nitrogen-doped carbon for room-temperature selective hydrogenation of nitroarenes. Chinese J Catal 39:664–672

13. Liao C, Liu B, Chi Q, Zhang Z (2018) Nitrogen-doped carbon materials for the metal-free reduction of nitro compounds. ACS Appl Mater Interface 10:44421–44429

14. Song J, Huang Z, Pan L, Li K, Zhang X, Wang L, Zou J (2018) Review on selective hydrogenation of nitroarene by catalytic, photocatalytic and electrocatalytic reactions. Appl Catal B Environ 227:386–408

15. Kumar A, Paul B, Boukherroub R, Jain SL (2020) Highly efficient conversion of the nitroarenes to amines at the interface of a ternary hybrid containing silver nanoparticles doped reduced graphene oxide/graphitic carbon nitride under visible light. J Hazard Mater 387:121700

16. Fukui M, Koshida W, Tanaka A, Hashimoto K, Kominami H (2020) Photocatalytic hydrogenation of nitrobenzenes to anilines over noble metal-free TiO2 utilizing methylamine as a hydrogen donor. Appl Catal B Environ 268:118446

17. Chen P, Khetan A, Yang F, Migunov V, Weide P, Stürmer S, Guo P, Kahler K, Xia W, Mayer J, Pitsch H, Simon U, Muhler M (2017) Experimental and theoretical understanding of nitrogen-doping-induced strong metal-support interactions in Pd/TiO2 catalysts for nitrobenzene hydrogenation. ACS Catal 7:1197–1206

18. Yin Z, Wang Y, Song C, Zheng L, Ma N, Liu X, Li S, Lin L, Li M, Xu Y, Li W, Hu G, Fang Z, Ma D (2018) Hybrid Au-Ag nanostructures for enhanced plasmon-driven catalytic selective hydrogenation through visible light irradiation and surface-enhanced raman scattering. J Am Chem Soc 140:864–867

19. Dai Y, Li C, Shen Y, Zhu S, Hvid M, Wu L, Skibsted J, Li Y, Niemantsverdriet J, Besenbacher F, Lock N, Su R (2018) Efficient solar-driven hydrogen transfer by bismuth-based photocatalyst with engineered basic sites. J Am Chem Soc 140:16711–16719

20. Hao C, Guo X, Pan Y, Chen S, Jiao Z, Yang H, Guo X (2016) Visible-light-driven selective photocatalytic hydrogenation of cinnamaldehyde over Au/SiC catalysts. J Am Chem Soc 138:9361–9364

21. Zhang L, He X, Xu X, Liu C, Duan Y, Hou L, Zhou Q, Ma C, Yang X, Liu R, Yang F, Cui L, Xu C, Li Y (2017) Highly active TiO2/g-C3N4/G photocatalyst with extended spectral response towards selective reduction of nitrobenzene. Appl Catal B Environ 203:1–8

22. Hao C, Guo X, Sankar M, Yang H, Ma B, Zhang Y, Tong X, Jin G, Guo X (2018) Synergistic effect of segregated Pd and Au nanoparticles on semiconducting SiC for efficient photocatalytic hydrogenation of nitroarenes, ACS Appl. Mater Interface 10:23029–23036

23. Zhao L, Wei J, Lu J, He C, Duan C (2017) Renewable molecular flasks with NADH models: combination of light-driven proton reduction and biomimetic hydrogenation of benzoxazinones. Angew Chem Int Ed 56:8692–8696

24. Xiao G, Li P, Zhao Y, Xu S, Su H (2018) Visible-light-driven chemoselective hydrogenation of nitroarenes to anilines in water through graphitic carbon nitride metal-free photocatalysis. Chem Asian J 13:1950–1955

25. Sharma P, Sasson Y (2019) Sustainable visible light assisted in situ hydrogenation via a magnesium-water system catalyzed by a Pd-g-C3N4 photocatalyst. Green Chem 21:261–268

26. Zhou B, Song J, Zhou H, Wu T, Han B (2016) Using the hydrogen and oxygen in water directly for hydrogenation reactions and glucose oxidation by photocatalysis. Chem Sci 7:463–468

27. Cao S, Chang J, Fang L, Wu L (2016) Metal nanoparticles confined in the nanospace of double-shelled hollow silica spheres for highly efficient and selective catalysis. Chem Mater 28:5596–5600

28. Zhang Y, Zhao Y, Cao S, Yin Z, Cheng L, Wu L (2017) Design and synthesis of hierarchical SiO2@C/TiO2 hollow spheres for high-performance supercapacitors. ACS Appl Mater Interface 9:29982–29991

29. Zhao S, Chen J, Liu Y, Jiang Y, Jiang C, Yin Z, Xiao Y, Cao S (2019) Silver nanoparticles confined in shell-in-shell hollow TiO2 manifesting efficiently photocatalytic activity and stability. Chem Eng J 367:249–259

30. Qi L, Sun Z, Tang Q, Wang J, Huang T, Sun C, Gao F, Tang C, Dong L (2020) Getting insight into the effect of CuO on red mud for the selective catalytic reduction of NO by NH3. J Hazard Mater 396:122459

31. Inui H, Takeda K, Kondo H, Ishikawa K, Sekine M, Kano H, Yoshida N, Hori M (2010) Measurement of hydrogen radical density and its impact on reduction of copper oxide in atmospheric-pressure remote plasma using H2 and Ar mixture gases. Appl Phys Express 3:126101

32. Gong H, Zhang Y, Cao Y, Luo M, Feng Z, Yang W, Liu K, Cao H, Yan H (2018) Pt@Cu2O/WO3 composite photocatalyst for enhanced photocatalytic water oxidation performance. Appl Catal B Environ 237:309–317

33. Han X, He X, Sun L, Zhan W, Xu J, Wang X, Chen J (2018) Increasing effective photogenerated carriers by in-situ anchoring Cu2O nanoparticles on nitrogen-doped porous carbon yolk-shell Cu boctahedral framework. ACS Catal 8:3348–335

34. Karthikeyan S, Kumar S, Durndell L, Isaacs M, Parlett C, Ben C, Douthwaite R, Jiang Z, Wilson K, Lee A (2018) Size-dependent visible light photocatalytic performance of Cu2O nanocubes. ChemCatChem 10:3554–3563

35. Zhang M, Chen Z, Wang Y, Zhang J, Zheng X, Rao D, Han X, Zhong C, Hu W, Deng Y (2019) Enhanced light harvesting and electron-hole separation for efficient photocatalytic hydrogen evolution over Cu7S4-enwrapped Cu2O nanocubes. Appl Catal B Environ 246:202–210

36. Zhang S, Yi JJ, Chen JR, Yin ZL, Tang T, Wei WW, Cao SS, Xu H (2020) Spatially confined Fe2O3 in hierarchical SiO2@TiO2 hollow sphere exhibiting superior photocatalytic efficiency for degrading antibiotics. Chem Eng J 380:122583

37. Toe C, Zheng Z, Wu H, Scott J, Amal R, Ng Y (2018) Photocorrosion of cuprous oxide in hydrogen production: rationalising self-oxidation or self-reduction. Angew Chem Int Ed 130:13801–13805

38. Wang C, Ma B, Xu S, Li D, He S, Zhao Y, Han J, Wei M, Evans D, Duan X (2017) Visible-light-driven overall water splitting with a largely-enhanced efficiency over a Cu2O@ZnCr-layered double hydroxide photocatalyst. Nano Energy 32:463–469

39. Dotan H, Sivula K, Grätzel M, Rothschild A, Warren S (2011) Probing the photoelectrochemical properties of hematite (α-Fe2O3) electrodes using hydrogen peroxide as a hole scavenger. Energy Environ Sci 4:958–964

40. Bhoi Y, Mishra B (2017) Single step combustion synthesis, characterization and photocatalytic application of α-Fe2O3-Bi2S3 heterojunctions for efficient and selective reduction of structurally diverse nitroarenes. Chem Eng J 31:70–81

41. Yin Z, Xiao Y, Li H, Chen G, Feng N, Wu J, Li H, Xu H, Cao S (2020) Metal nanoparticles confined within inorganic-organic framework enables superior substrate-selective catalysis. ACS Appl Mater Interfaces 12:42739–42748

42. Liu Y, Zhang B, Luo L, Chen X, Wang Z, Wu E, Su D, Huang W (2015) TiO2/Cu2O core/ultrathin shell nanorods as efficient and stable photocatalysts for water reduction. Angew Chem Int Ed 54:15260–15265

43. Tsutsumi K, Uchikawa F, Sakai K, Tabata K (2016) Photoinduced reduction of nitroarenes using a transition-metal-loaded silicon semiconductor under visible light irradiation. ACS Catal 6:4394–4398

44. Yin Z, Xie L, Cao S, Xiao Y, Chen G, Jiang Y, Wei W, Wu L (2020) Ag/Ag2O confined visible-light driven catalyst for highly efficient selective hydrogenation of nitroarenes in pure water medium at room temperature. Chem Eng J 394:125036

Supplementary data

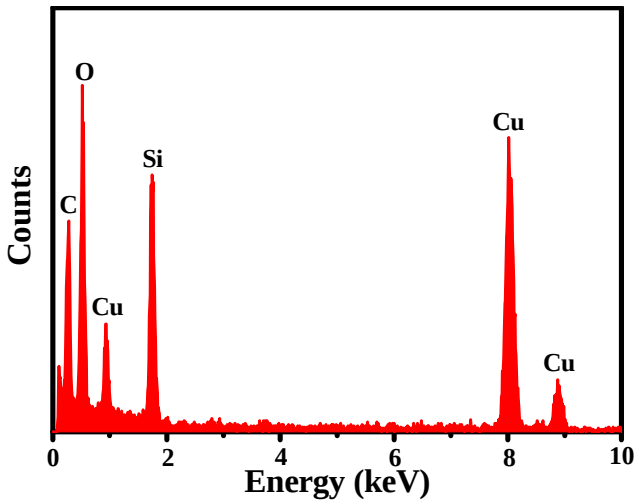

Fig.S1 EDX of as-synthesized SiO_2-Cu_2O@SiO_2 sample

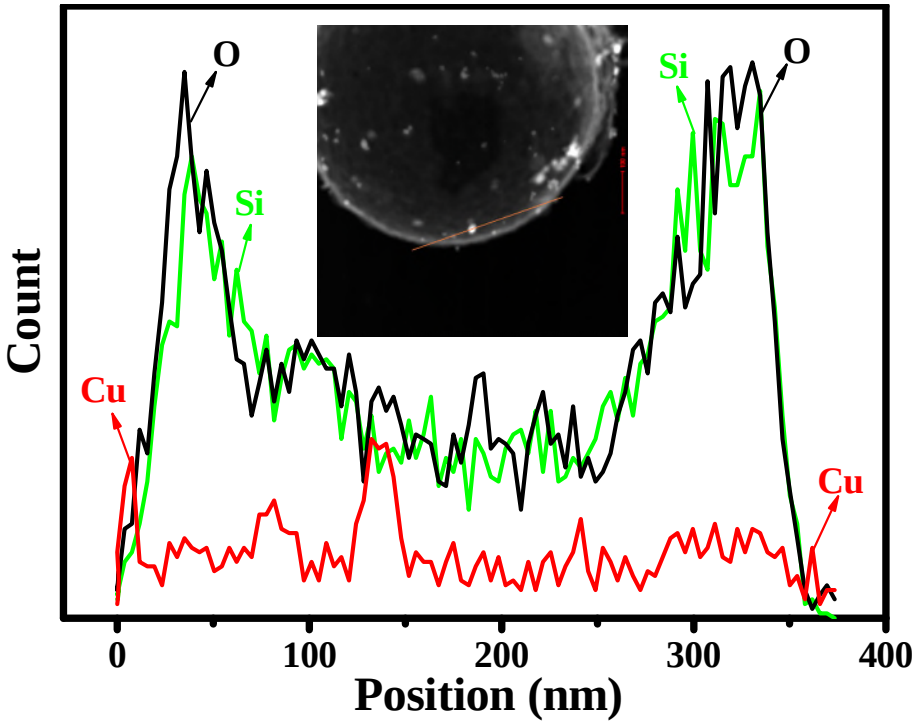

Fig.S2 Elemental profiles (Si, O, and Cu elements) of surface-supported Cu_2O (SiO_2-Cu_2O) sample

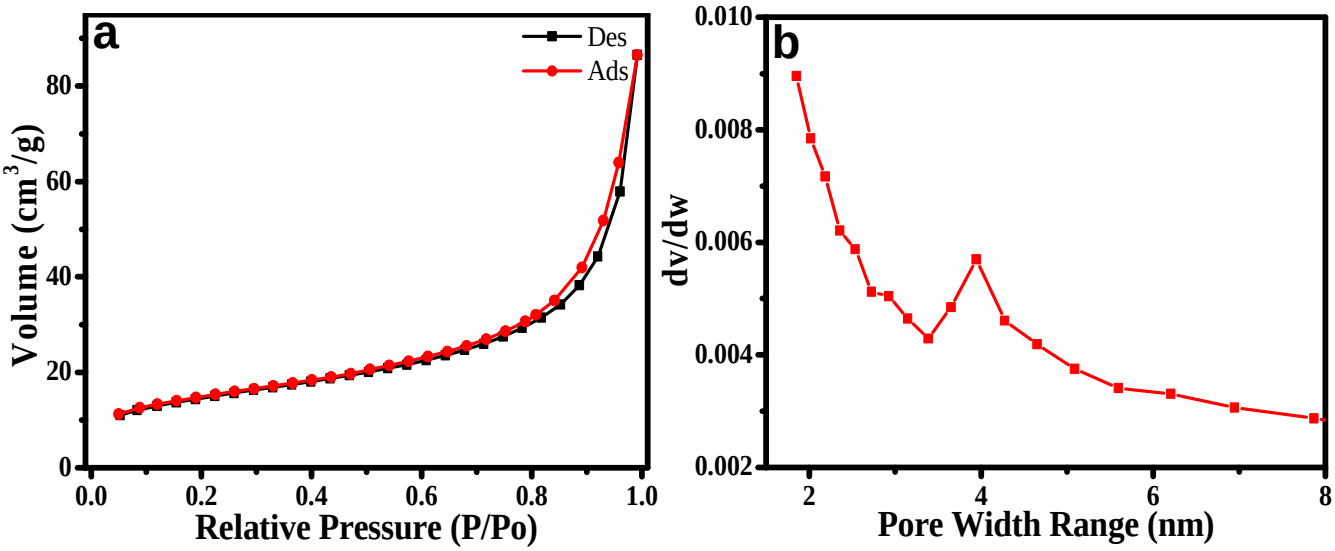

Fig.S3 N_2 adsorption-desorption isotherm (a) and pore size distribution (b) of the as-synthesized SiO_2-Cu_2O@SiO_2 photocatalyst

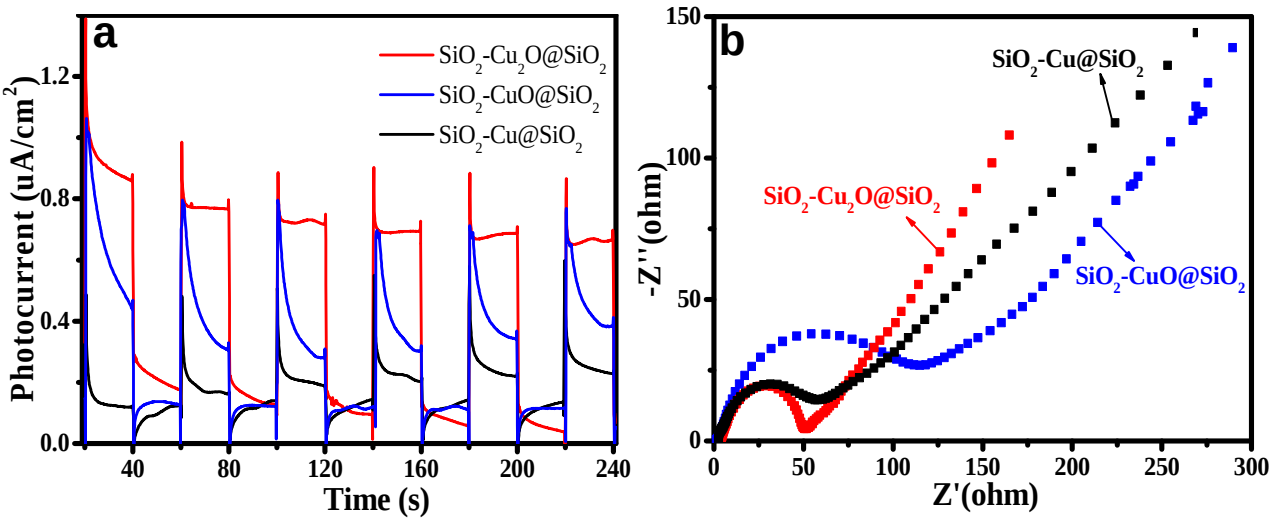

Fig.S4 transient photocurrent response of three photocatalysts (a), EIS Nyquist plots of the electrodes (b)

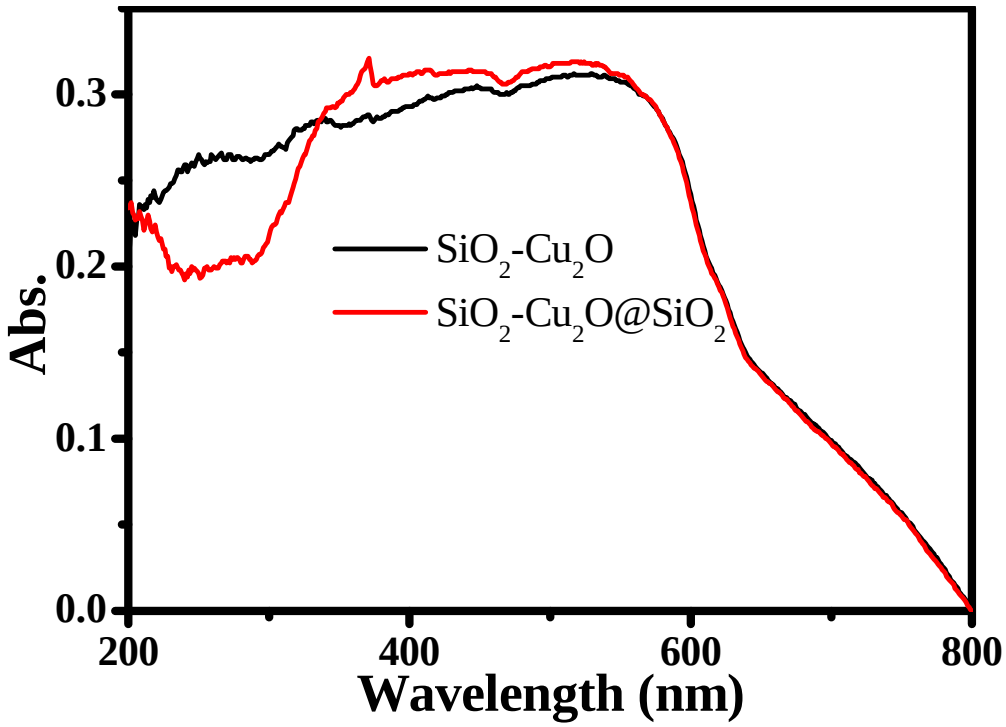

Fig.S5 Uv-vis spectra of the confined SiO_2-Cu_2O@SiO_2 and surface-supported SiO_2-Cu_2O samples

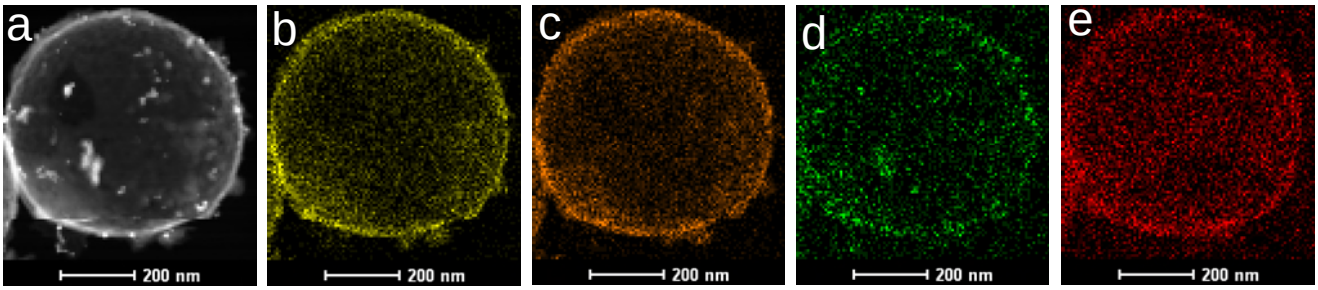

Fig.S6 (a) STEM images and EDX mapping (b: Si, c: O,d: Cu, and e: C) of hierarchically hollow SiO_2-Cu_2O spheres

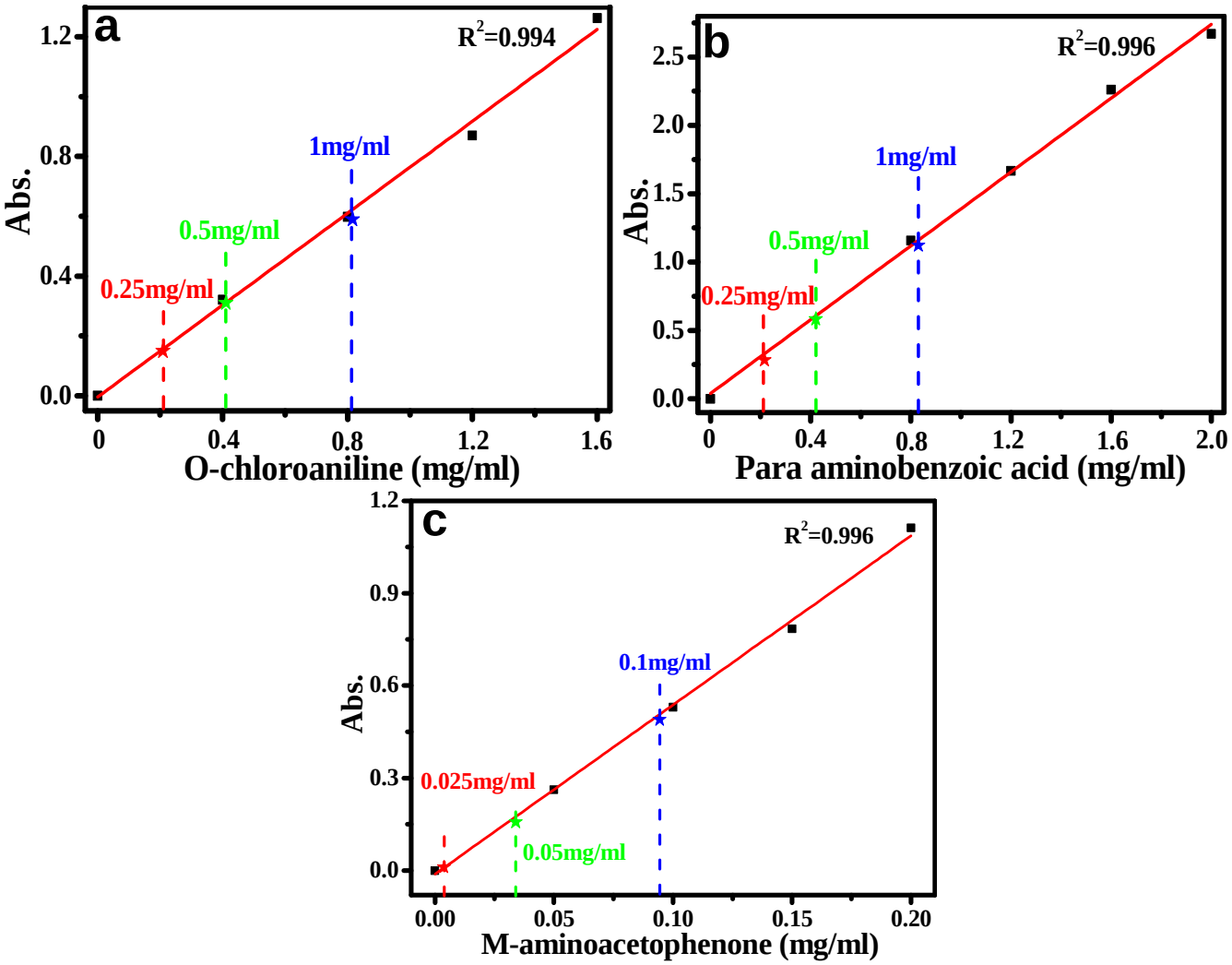

Fig.S7 The corresponding aniline (star) obtained towards the hydrogenation of nitroarenes and commercial aniline (black dots).

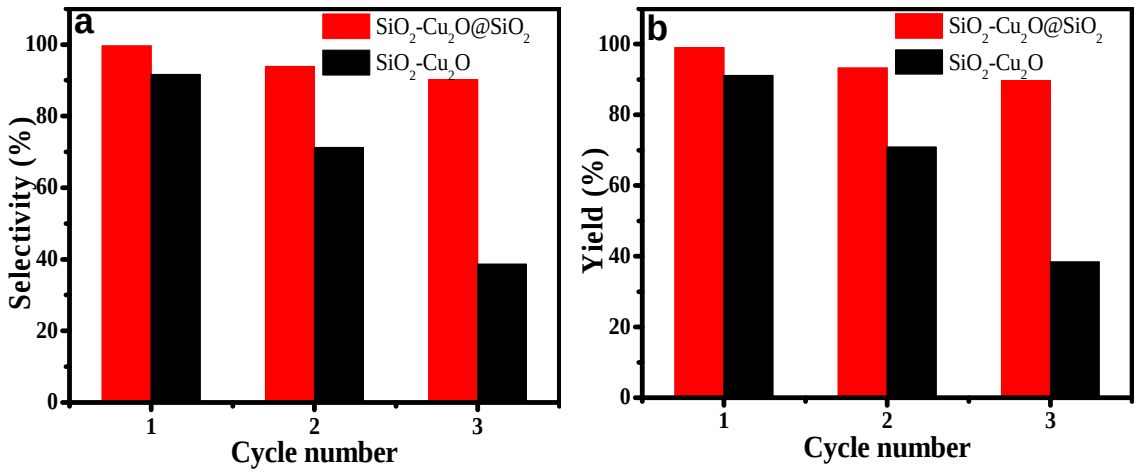

Fig.S8 Cycle stabilities of the confined SiO_2-Cu_2O@Si_2O and surface-supported SiO_2-Cu_2O samples

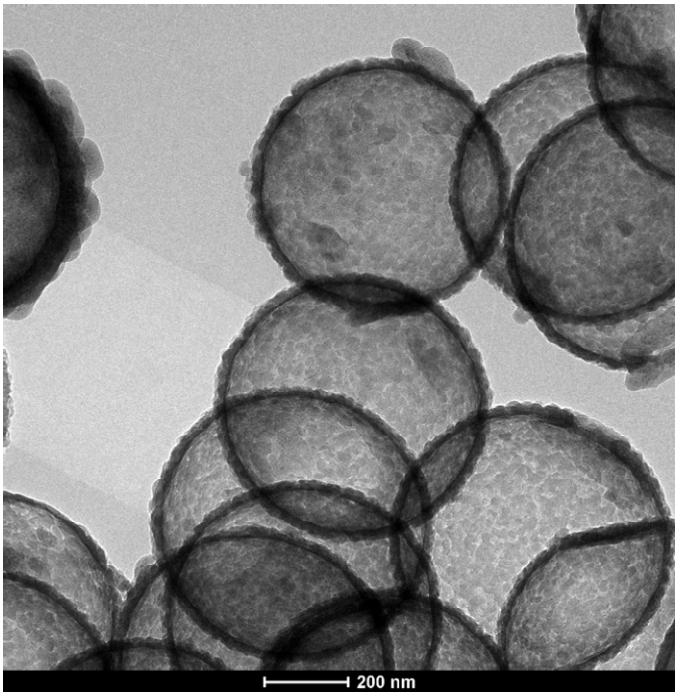

Fig.S9 TEM image of the confined SiO_2-Cu_2O@Si_2O sample after third cycle

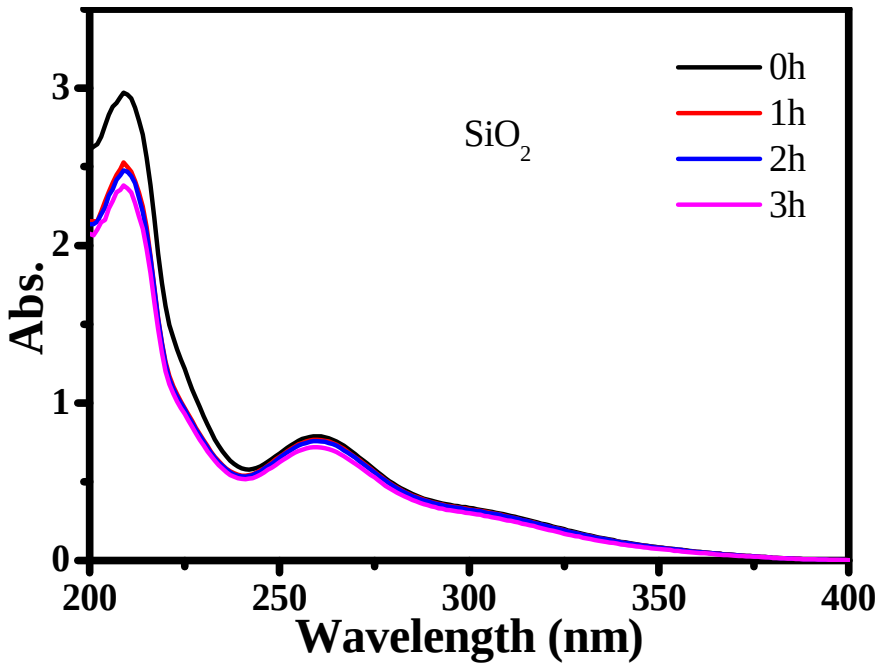

Fig.S10 UV-vis spectra of the aqueous solutions of o-NCB over hierarchically hollow SiO_2 spheres under visible-light irradiation

Table S1. The photocatalytic activity of catalysts for the hydrogenation of nitroarenes in aqueous system

Nitroarene	SiO_2-Cu_2O@SiO_2			SiO_2-CuO@SiO_2			SiO_2-Cu@SiO_2		
	Conv (%)	Selec (%)	Yield (%)	Conv (%)	Selec (%)	Yield (%)	Conv (%)	Selec (%)	Yield (%)
o-NCB (0.25 mg/ml)	100	100	99.6	77.8	77.4	76.9	81.7	80.6	80.1
p-NBA (0.25 mg/ml)	100	100	99.9	68.4	67.1	66.8	64.5	66.1	65.8
i-NAP (0.025 mg/ml)	100	100	99.6	71.6	68.9	68.6	58.4	57.7	57.5

Table S2. The photocatalytic activity of catalysts for the hydrogenation of nitroarenes in aqueous system

Nitroarene	SiO_2-Cu_2O@SiO_2			SiO_2-CuO@SiO_2			SiO_2-Cu@SiO_2		
	Conv (%)	Selec (%)	Yield (%)	Conv (%)	Selec (%)	Yield (%)	Conv (%)	Selec (%)	Yield (%)
o-NCB (0.5 mg/ml)	100	100	99.6	65.4	63.1	62.7	73.3	73.1	72.7
p-NBA (0.5 mg/ml)	100	99.9	99.3	59.1	58.4	58.2	61.0	60.3	60.1
i-NAP (0.05 mg/ml)	100	99.7	99.3	61.3	57.4	57.2	53.9	51.0	50.8

Table S3. Comparative photocatalytic performances of typically reported photocatalysts and this work

Catalyst	Reaction medium	Light source	Time/ Temperature	Substance	Yield (%)	Ref
$Au_{2.6}Cu_{0.4}$@ZrO_2	isopropyl alcohol/KOH	λ > 400 nm	6h/40□	p-nitroacetophenone	89	[1]
$Cu_{1.94}S$-$Zn_{0.23}Cd_{0.77}S$	methanol/ H_2O,Na_2S, Na_2SO_3	λ > 420 nm	110min/ 10±0.2□	4-chloronitrobenzene	80	[2]
AuPt/TN	methanol/ $HCOONH_4$	λ≤ 800	4h/RT	4-chloronitrobenzene	>99	[3]
Pd/Ag/SBA-15(Pd/Ag/ SiO_2	ethanol/H_2O/AB	Visible Light	160min/RT	p-nitrostyrene	89	[4]
$Pd_3Au_{0.5}$/SiC	ethanol	Visible Light	30min/25□	4-chloronitrobenzene	100	[5]
Pt/CdS	Benzotrifluoride	λ > 420 nm	4h/40□	4-chloronitrobenzene	<70	[6]
Fe_2O_3-Bi_2S_3	$N_2H_4{\cdot}H_2O$	λ > 420 nm	4h/	4-chloronitrobenzene	91	[7]
Pd/TiO_2	H_2O	UV-ligh	10-20h/ 25□	4-chloronitrobenzene	>95	[8]
g-C_3N_4	H_2O	Visible Light	18h/90□	2-nitrochlorobenzene	88	[9]
Pd-g-C_3N_4	H_2O	λ > 420 nm	12h/RT	p-nitrobenzoic	>90	[10]
SiO_2-Cu_2O@SiO_2	H_2O (10ml)	λ > 400 nm	3h/RT	2-nitrochlorobenze p-nitrobenzoic m-nitroacetophenone	>99	Our work

References

[1] Q. Xiao, S. Sarina, Eric R. Waclawik, J. Jia, J. Chang, James D. Riches, H. Wu, Z. Zheng, H. Zhu, ACS Catal. **6**, 1744-1753 (2016).

[2] Z. Yu, Z. Chen, Y. Chen, Q. Peng, R.Lin, Y. Wang, R. Shen, X. Cao, Z. Zhuang, Y. Li, Nano Research. **11**, 3730-3738 (2018).

[3] Y. Song, H. Wang, Z. Wang, B. Guo, K. Jing, Y.Li, L. Wu, ACS Catal. **8**, 9656-9664 (2018).

[4] P. Verma, Miriam NavlaniGarca, Y. Kuwahara, K. Mori, H. Yamashita, J. Chem. Sci. **129**, 1661-1669 **(**2017).

[5] C. Hao, X. Guo, M. Sankar, H. Yang, B. Ma, Y. Zhang, X. Tong, G. Jin, X. Guo, ACS Appl Mater Inter. **10**, 23029-23036 (2018).

[6] S. Zhang, W. Huang, X. Fu, G. Chen, S. Meng, S. Chen, J. Hazard. Mater. **360**, 182-192 (2018).

[7] Y.P. Bhoi, B.G. Mishra, Chem. Eng. J. **316**, 70-81 (2017).

[8] B. Zhou, J. Song, H. Zhou, T. Wu, B. Han, Chem Sci**. 7**, 463-468 (2016).

[9] G. Xiao, P.Li, Y. Zhao, S.Xu, H. Su, Chem. Asian J**. 13**, 1950-1955 (2018).

[10] P. Sharma, Y. Sasson, Green Chem**. 21**, 261-268 (2019).

High photocatalytic activity of Cu2O embedded in hierarchically hollow SiO2 for efficient chemoselective hydrogenation of nitroarenes

Yin, Zhengliang

2020-10-20

Yin Z, Xiao Y, Wan X, et al., (2020) High photocatalytic activity of Cu2O embedded in hierarchically hollow SiO2 for efficient chemoselective hydrogenation of nitroarenes. Journal of Materials Science, Volume 56, February 2021, pp. 3874-3886

https://doi.org/10.1007/s10853-020-05449-x